Mathematical Theory and Modeling
ISSN 2224-5804 (Paper) ISSN 2225-0522 (Online)
Vol.8, No.2, 2018
www.iiste.org

SIMULATION AND CONTROL OF A REACTOR FOR THE NON-CATALYTIC HYDROLYSIS OF ETHYLENE OXIDE TO ETHYLENE GLYCOL

[1]Akpa, Jackson Gunorubon, Onuorah, Paschal[2]
Department of Chemical/Petrochemical Engineering
Rivers State University,
Port-Harcourt, Rivers State, Nigeria
[1](corresponding author: akpa.jackson@ust.edu.ng), [2](onuorahpaschal@gmail.com)

Dynamic Models for predicting the concentration profiles of a Continuous Stirred Tank Reactor for the Non-Catalytic hydrolysis of Ethylene Oxide to Mono Ethylene Glycol (MEG) have been developed. The models validated by solving model equations using ode45 solver of Mathlab 7.5 with industrial plant data from Batiha, (2004a) had a deviation of 2.47% and 0.93% for ethylene oxide and water respectively when the model outputs were compared with the industrial plant outputs. Simulations of reactor to ($\pm$) step changes in the inlet flowrates showed great effect on Mono-Ethylene Glycol production. The dynamic models were used for control studies by incorporating a Proportional-Integral-Derivative (PID) feedback Controller. The closed loop response of the reactor output showed continuous oscillatory response with offset. Hence the controller parameters (proportional gain K_c, Integral time τ_I and derivative time τ_D) were tuned using the 'On-Line Trial and Error Method' implemented using MathLab Simulink to obtain optimum values that ensured quick stability of the closed-loop system, reduced or no oscillatory response and no offset. The optimum controller parameter: proportional gain $K_c = 0.1$, Integral time $\tau_I = 14$ and derivative time τ_D = 3 were obtained and the reactor attained stability in about 180 seconds
key words: simulation, control, Ethylene Glycol production, reactor model

1. Introduction

Ethylene Glycol (Ethane -1, 2- diol) is an organic compound primarily used in the manufacture of Polyester, Fibres, Fabric, solvents for paints and plastics, as hydraulic brake fluids and in the preparation of Polyethylene Terephthalate (PET) resin used in making plastic bottles for soft drinks (Landau & Ozero, 1982). Ethylene Glycol can be manufactured industrially via the catalytic process where the reaction is catalysed by either an acid or base or the non-catalytic process where the reaction occur at neutral pH and at elevated temperatures.

The direct un-catalyzed neutral hydrolysis of ethylene oxide to ethylene glycol at high temperature is the most widely used method (Samoilov & Mnushkin, 2012); in this process, ethylene oxide is converted to ethylene glycol through uncatalyzed neutral (pH 6 –10)

hydrolysis (with excess water) at high temperatures and pressures (Rebsdat and Mayer 2005). The primary product is mono-ethylene glycol (MEG) with higher glycols such as di and tri ethylene glycols (DEG and TEG) formed in smaller amounts as the reaction proceeds through a series of consecutive – parallel reactions. The use of excess water to control selectivity towards Mono-ethylene glycol has been reported by Yang, et al., (2010) to increase production cost due to high energy consumption during the distillation process to remove water. The use of efficient catalysts that uses low water/ethylene oxide ratio, thus reduce cost; has also been reported - catalytic processes where Ethylene Oxide is hydrolyzed over various catalyst to produce ethylene glycol. These processes incudes ethylene oxide hydrolysis over: Phosphorus-based Halide Catalysts (Kawabe, 2000); anion exchange resins such as halogenate or bicarbonate-type: Strickler *et al*, (1999); polymer of a vinylaromatic compound: Iwakura and Miyagi, (2000); HCO_3^-/CO_3^{2-} catalyst form: Shvets, et al., (2005); supported metal oxides and zeolites: Li, et al., (2004), Li, et al., (2005), Li, et al., (2006); polymeric organosilane ammonium salts: Kruchten, (1999a) and macrocyclic chelating compounds: Kruchten, (1999b). Other production methods include the direct oxidation of ethylene and synthesis from carbon monoxide (Rebsdat and Mayer 2005) and the direct catalytic hydrolysis of methanol and its derivatives such as formaldehyde to ethylene glycol (Celik et al., 2008), this method has been reported to be cheaper as the carbon needed for this process is derived from synthesis gas (obtained from natural gas, coal, or biomass), a cheaper carbon source than petroleum-derived ethylene. A typical process scheme shown in Figure 1 is complex consisting of a reactor, an evaporator and columns/vaporizers amongst other equipment. Samoilov, & Mnushkin, (2012) proposed the use of a single apparatus – the reactive distillation column for this process.

1.1. Process Description: Hydrolysis of Ethylene Oxide

A flow diagram of the manufacture of ethylene glycol through the un-catalyzed hydrolysis of ethylene Oxide (Arrieta, 2001) is shown in Figure 1.

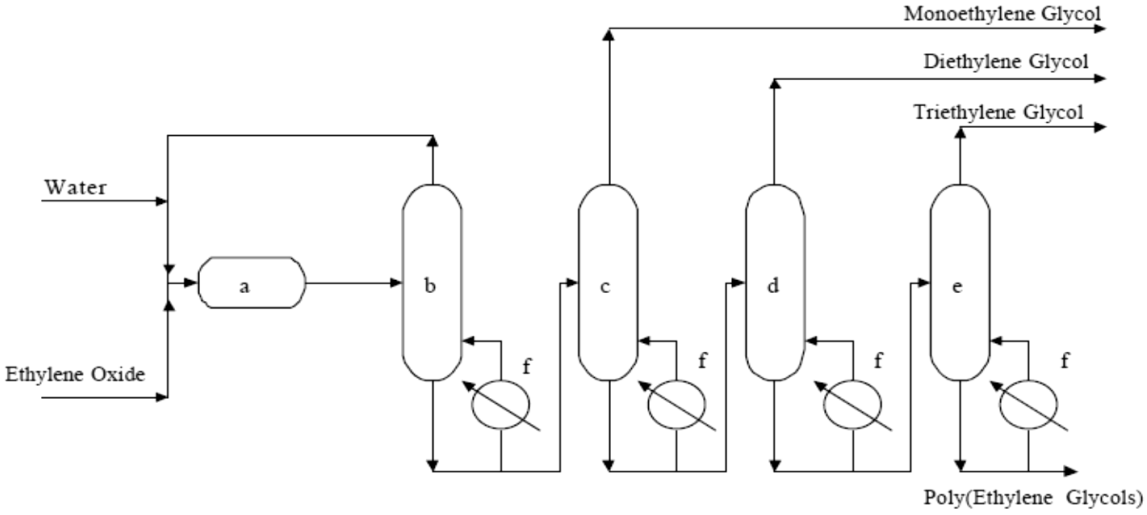

Figure 1: Flow diagram for a plant for hydrolysis of Ethylene Oxide (Arrieta, 2001).
a. Reactor b. Evaporator c. MEG Column d. DEG Column e. TEG Column f. Reboilers

Ethylene Oxide stream is first contacted with Water in a gas absorber at an Ethylene Oxide (EO) to Water ratio of about 1:20 (to reduce the formation of higher homologues). The Ethylene Oxide solution is preheated to a temperature of about 200^{o}C and fed to a Continuous Stirred Tank reactor (CSTR) where it is thermally hydrolyzed to Ethylene Glycol at an operating temperature of about 190 – 200^{o}C and pressure of about 14 – 22 atm. Ethylene Oxide reacts further with Mono-ethylene Glycol (MEG) and higher homologues in a series – parallel reaction to form di-ethylene and tri-ethylene glycol. The Water – Ethylene Glycol mixture from the reactor is fed to the first stage of a multi-stage evaporator, where it is re-boiled using high-pressure steam then sent to a sequence of columns where the ethylene glycol is separated to mono, di, and tri ethylene glycol respectively.

Ethylene Oxide reacts faster with Ethylene Glycol than it does with Water (Melhem, et al., 2001), hence without control, reaction proceeds normally with the successive formation of

higher homologues of glycol (di, tri, tetra ethylene glycol) through the continuous reaction of ethylene oxide with the ethylene glycol homologue formed – by addition polymerization to form higher ethylene glycols. The most important process variable affecting the glycols (mono, di or tri ethylene glycol) distribution is the water to ethylene oxide ratio in the starting material and only marginally on the reaction pH and temperature (Rebsdat & Mayer, 2005). Hence an excess of water is usually used in commercial plants (almost 20 times more) for high selectivity and to achieve at least a 90% conversion of Ethylene Oxide to mono ethylene glycol (MEG) (Arrieta, 2001).

Therefore, to stop the continuous reaction, ensure selectivity and maximum mono ethylene production (maximum volume for MEG), it is expedient that some form of control mechanism be implemented to maintain the required Ethylene Oxide to Water ratio of the feed entering the reactor. That is – maintain maximum volume of the mono ethylene glycol (MEG) measured by the MEG/liquid level in the reactor (output variable) as changes in the disturbance - inlet flowrate of the reactants occurs by manipulating the ethylene oxide to water ratio – the manipulated variable. This involves the installation of appropriate controller which returns the output variable back to its set point value whenever there is a disturbance (changes in the inlet flowrate) in the process. Hence this work studied the behavior of the continuous stirred tank reactor (CSTR) used for the hydrolysis of ethylene oxide to ethylene glycol particularly to fluctuations in the feed flowrate and develop appropriate closed loop models with Proportional-Integral-Derivative Controller capable of bringing the system back/close to its original set point value and ensure stability of the process.

2. Material and Methods

2.1. Methods

The mathematical models of the continuous stirred tank reactor (CSTR) were developed by applying the principle of conservation of mass and energy on the reactor. These models (open

loop process models) were ordinary differential equations and were solved with industrial process data from Batiha, (2004a) and model parameters from Sinnott & Towler, (2009) using the ode45 solver from MATLAB 7.5.0. The open loop models were simulated to determine the effects of step-changes of $\pm$25% and $\pm$50% in the feed flowrate on the reactor performance – the quantity or volume of mono ethylene glycol produced. The control objective was to ensure maximum production (volume) of MEG in the reactor which was measured by the liquid/mono ethylene glycol (MEG) height/level for a reactor of constant cross-sectional area as fluctuations in the inlet flowrate occur. This was achieved by manipulating the feed inlet flowrate through the ethylene oxide – water ratio of the feed. The feedback control configuration with Proportional-Integral-Derivative (PID) controller was used to effect the control action. A closed loop block diagram of the process was developed from which the closed loop model of the process output (MEG height) was developed. The closed loop model equation of the process was developed in terms of the transfer functions of the components of the closed loop block diagram. The close loop model was used to study the effects of the PID controller to step changes in the inlet flowrate on the liquid (MEG) level in the reactor. To effectively ensure this control – minimize the effects of disturbances, obtain rapid and smooth responses to set point changes with little or no oscillations and eliminate steady state error (offset); the optimum values of the controller parameters (controller gain K_C, the integral or reset time τ_I and the derivative time τ_D) had to be determined (controller tuning) - a systematic selection of controller parameter values that achieves control objectives; an iterative procedure using the On-Line Trial and Error Method (Luyben, 1990) implemented with MathLab Simulink was developed. In this procedure, several/different combinations of the controller's parameters values were used in solving the closed loop model to obtain the response of the output/controlled variable (liquid/MEG level) to ($\pm$) step changes in the disturbance (inlet feed flowrate). The combination values of these parameters

that stabilizes the output (MEG level) in the reactor, nullifies the effect of the disturbance - maintains a constant/maximum value of the liquid/MEG level (the desired/set point value) is the optimum and required controller setting for effective control of the process.

2.2. Model Development

2.2.1. Kinetic Model

The elementary steps of the series-parallel reactions for the non-catalytic process of Ethylene Glycol synthesis are as follows - reaction of Ethylene Oxide with water to give Mono Ethylene Glycol (MEG) and subsequent reaction with ethylene oxide to form di and tri ethylene glycol:

$$C_2H_4O + H_2O \xrightarrow{K_1} C_2H_6O_2 \quad (1)$$

$$C_2H_4O + C_2H_6O_2 \xrightarrow{K_2} C_4H_{10}O_3 \quad (2)$$

$$C_2H_4O + C_4H_{10}O_3 \xrightarrow{K_3} C_6H_{14}O_4 \quad (3)$$

The rate expressions for any component j from equations (1), (2) and (3) can be written

For j = A,B,C,D, E: A represent C_2H_4O; B: water; C: $C_2H_6O_2$; D: $C_4H_{10}O_3$; E: $C_6H_{14}O_4$ as:

$$(-r_A) = -K_1C_AC_B - K_2C_AC_C - K_3C_AC_D \quad (4)$$

$$(-r_B) = -K_1C_AC_B \quad (5)$$

$$(r_c) = K_1C_AC_B - K_2C_AC_C \quad (6)$$

$$(r_D) = K_2C_AC_C - K_3C_AC_D \quad (7)$$

$$(r_E) = K_3C_AC_D \quad (8)$$

The reaction rate constant (K_i) for any reaction path i is Arrhenius law dependent given as:

$$K_i = k_{i_0}e^{-\frac{E_i}{RT}} \quad (9)$$

The rate constant for reaction 1 as a function of temperature is given by Batiha, (2004b):

$$K_1 = 7.123E + 08 \times exp\left(\frac{-21193}{RT}\right) \quad (10)$$

The ratios of the rate constants for the reaction paths as given by Batiha, (2004b) are:

$$\frac{K_2}{K_1} = 2.946, \qquad \frac{K_3}{K_1} = 3.229 \tag{11}$$

2.2.2. Reactor Model

The following simplifying assumptions were made in the development of the process model: The reactants are perfectly mixed, hence outlet and inlet condition of the reactor are the same, density is constant and heat capacity varies negligibly with temperature, the reactor is perfectly insulated and there is no heat loss. The continuous stirred tank reactor used for the hydrolysis reaction is represented by a single input - single output system as shown in Figure

C_{j_o}, q_i, T_i

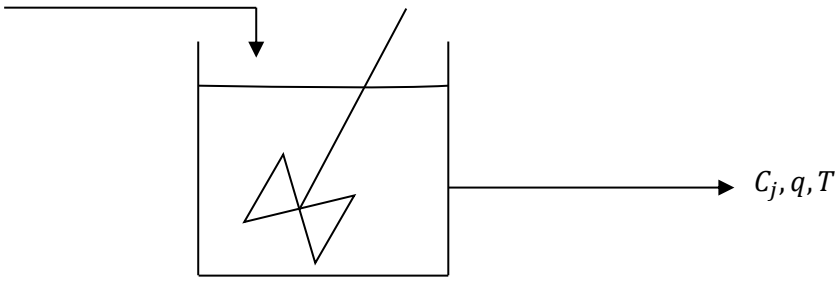

Figure 2: Schematic of the CSTR

The Continuous Stirred Tank Reactor (CSTR) model was obtained by applying the conservation principle on the fundamental quantities which characterize the system: Total mass, Component mass and Total Energy as follows:

i. Total mass balance

A Total mass balance on the CSTR gives:

$$\frac{d(\rho V)}{dt} = \rho_i q_i - \rho q \tag{12}$$

But $\rho_i = \rho; \quad V = Ah,$

Substituting and rearranging gives:

$$A\frac{dh}{dt} = q_i - q \tag{13}$$

ii. Component mass Balance

A component mass balance for any component (j) of the CSTR yields:

$$\frac{d(VC_j)}{dt} = q_i C_{jo} - qC_j + (r_j)V \tag{14}$$

substituting $V = Ah$ and expanding gives:

$$A\left[h\frac{dC_j}{dt} + C_i\frac{dh}{dt}\right] = q_i C_{jo} - qC_j + (r_j)Ah \tag{15}$$

Substituting equation (13), rearranging and simplifying gives:

$$\frac{dC_j}{dt} = \frac{q_i}{Ah}(C_{jo} - C_j) + (r_j) \tag{16}$$

iii. Energy Balance

The principle of Conservation of energy applied on the reactor gives:

$$\frac{d(\rho VC_pT)}{dt} = \rho q_i C_P T_i - \rho q C_P T + (-\Delta H_r)(r_j)Ah \tag{17}$$

Expanding and assuming ρ and C_P vary negligibly with temperature, equation becomes:

$$\rho AC_P\left[\frac{hdT}{dt} + \frac{Tdh}{dt}\right] = \rho C_P(q_i T_i - qT) + (-\Delta H_r)(r_j)Ah \tag{18}$$

Substituting eqn. (13) and simplifying gives:

$$\frac{dT}{dt} = \frac{q_i}{Ah}(T_i - T) + \frac{(-\Delta H_r)}{\rho C_P}(r_j) \tag{19}$$

2.3. Process Control

The Control Objective was to ensure the liquid/MEG level in the reactor is maintained at a maximum pre specified level (is stable - does not fluctuate with time) in the face of ever-changing disturbances (step changes in the inlet flow rate – a *Servo* problem). The Closed loop diagram of the process is shown in Figure 3.

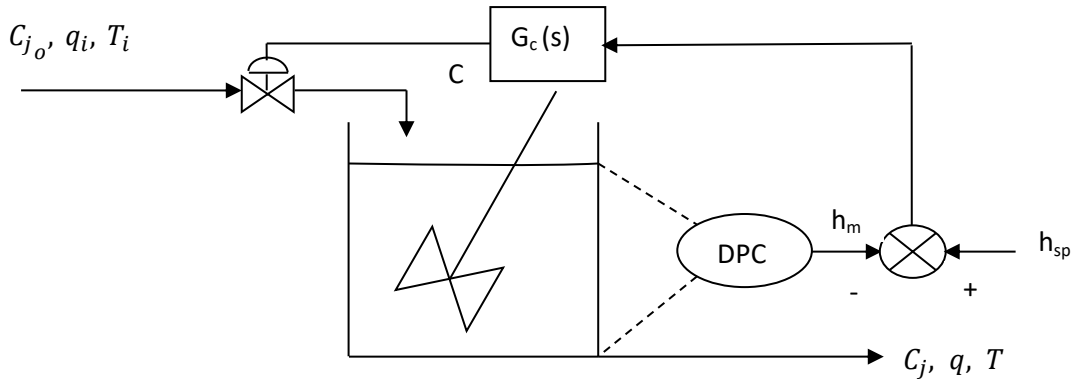

Figure 3: Closed-Loop diagram of the Process.

*DPC – Differential Pressure Cell

The general model equation for the output (liquid/MEG level, $h_{(S)}$) of the closed loop process in the Laplace domain due to set point ($h_{SP(S)}$) and load/disturbance ($d_{(s)}$) changes in terms of transfer functions of the various components in Figure 3 was developed to give:

$$h_{(S)} = \frac{G_{f(s)}\, G_{c(s)}\, G_{p(s)}}{1+ G_{f(s)}\, G_{c(s)}\, G_{m(s)}\, G_{p(s)}}\, h_{SP(S)} + \frac{G_{d(s)}}{1+ G_{f(s)}\, G_{c(s)}\, G_{m(s)}\, G_{p(s)}}\, d_{(s)} \qquad (20)$$

For the servo control problem where the load does not change ($d_{(s)}$= 0), while the set point undergoes step changes; the feedback controller acts to keep the liquid level ($h_{(S)}$) close to the set point (maximum MEG height) ($h_{SP(S)}$). The output $h_{(S)}$ from equation (20) becomes:

$$h_{(S)} = \frac{G_{f(s)}\, G_{c(s)}\, G_{p(s)}}{1+ G_{f(s)}\, G_{c(s)}\, G_{m(s)}\, G_{p(s)}}\, h_{SP(S)} \qquad (21)$$

The transfer function of each component was obtained by expressing the component model equation in deviation variables form, laplace trasform the resulting equation and rearrange the final equation in the input-output form. The transfer function for the various components in the closed loop diagram (Figure 3) were therfore obtained following this procedure as follows:

i. Process

The model of the liquid level at any time for a P% magnitude step change in inlet flowrate is given as:

$$A\frac{dh}{dt} = Pq_i - Ah \tag{22}$$

where: $q = Ah$

This equation can be written in terms of deviation variables and rearranged as:

$$A\frac{dh'}{dt} + Ah' = Pq'_i \tag{23}$$

Taking the Laplace transform and rearranging equation gives the Transfer function as:

$$G_p(s) = \frac{\bar{h}'(s)}{q'_i(s)} = \frac{P}{A(S+1)} \tag{24}$$

ii Controller: Proportional-Integral-Derivative (PID) Controller

The model equation for the controller in deviation variables is:

$$\bar{C}'(t) = K_c\left(\bar{\varepsilon}'(t) + \frac{1}{\tau_I}\int_0^t \bar{\varepsilon}'(t)dt + \tau_D\frac{d\bar{\varepsilon}'(t)}{dt}\right) \tag{25}$$

Equation (25) was laplaced and rearranged to obtain the Transfer function as:

$$G_c(s) = \frac{\bar{C}'(s)}{\bar{\varepsilon}'(s)} = K_c\left(1 + \frac{1}{\tau_I s} + \tau_D s\right) \tag{26}$$

iii Measuring Device (Differential Pressure Cell)

The mathematical models for the Differential Pressure Cell; Stephanopoulos, (2012) is:

$$\left(\frac{AL\rho}{Kg_c}\right)\frac{d^2x}{dt^2} + \frac{C}{K}\frac{dx}{dt} + x = \frac{A}{K}\Delta P \tag{27}$$

Where, A = Cross-sectional area of the Capillary tube,

L = Length of the Capillary Tube,

ρ = Density of the Liquid,

x = Fluid displacement in the Capillary Tube,

K = Hooke's constant for the Diaphragm,

g_c = Conversion Constant,

C = Damping Coefficient,

ΔP = Differential pressure across the cell.

This equation shows that the system's response follows a second-order dynamics and can be written in standard form as:

$$\tau^2 \frac{d^2x}{dt^2} + 2\zeta\tau \frac{dx}{dt} + x = K_P \Delta P \quad (28)$$

Where: $\tau^2 = \left(\frac{AL\rho}{Kg_c}\right)$, $2\zeta\tau = \frac{C}{K}$, $K_P = \frac{A}{K}$

If $x = h_m$; $\Delta P = \beta h$ equation becomes:

$$\tau^2 \frac{d^2h_m}{dt^2} + 2\zeta\tau \frac{dh_m}{dt} + h_m = K_P \beta h \quad (29)$$

This equation was expressed in deviation variables, Laplace transformed and rearranged to obtain the transfer function as:

$$G_m(s) = \frac{\bar{h}_m(s)}{\bar{h}(s)} = \frac{K_P\beta}{(\tau^2 s^2 + 2\zeta\tau s + 1)} \quad (30)$$

iv Final Control Element (The Control Valve)

Process Control Valves are designed so that the flow rate through the valve is a nearly linear function of the signal to the valve's actuator. A first-order transfer function provides an adequate model for an installed valve (Stephanopoulos, 2012) as:

$$\bar{h}'(s) = \frac{K_v}{\tau_v s + 1} \bar{C}'(s) \quad (31)$$

Hence the Transfer function is:

$$G_f(s) = \frac{\bar{h}'(s)}{\bar{C}'(s)} = \frac{K_v}{\tau_v s + 1} \quad (32)$$

The block diagram for the closed-loop system with the transfer functions is shown in Figure 4:

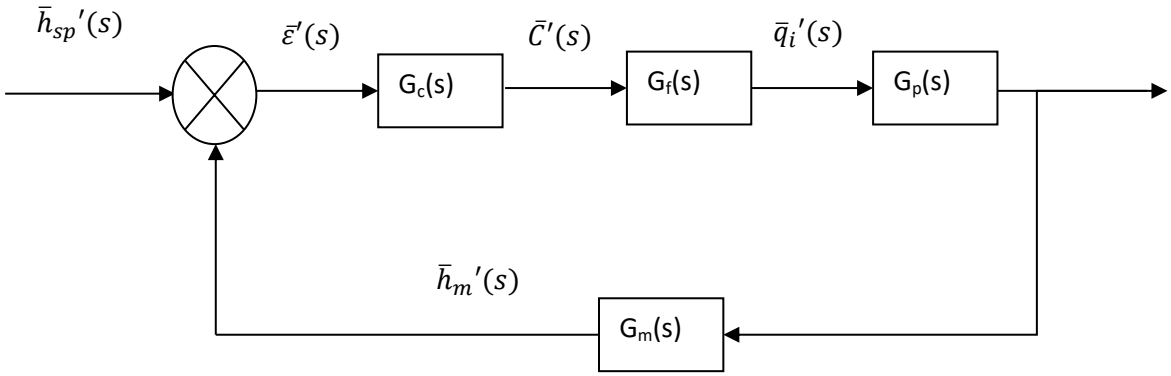

Figure 4: Block Diagram of Closed-Loop System

3. Discussion of Results

3.1. Open Loop Response

The concentrations of the reactants as predicted by a solution of the model equations are shown in Figures 5 and 6.

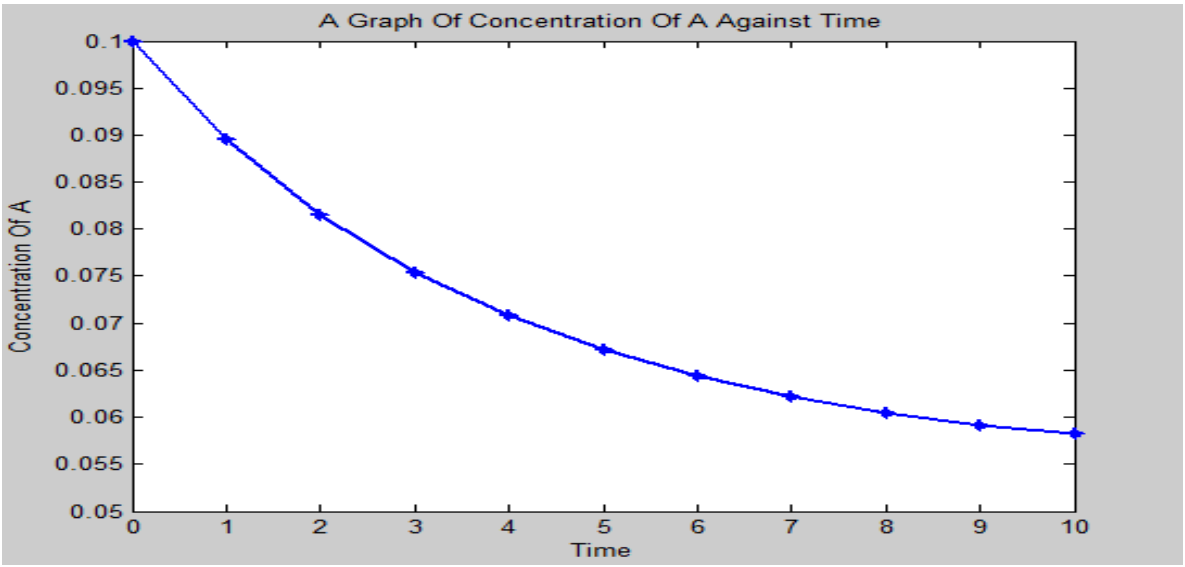

Figure 5: Plot of Variation in concentration of Ethylene Oxide with time.

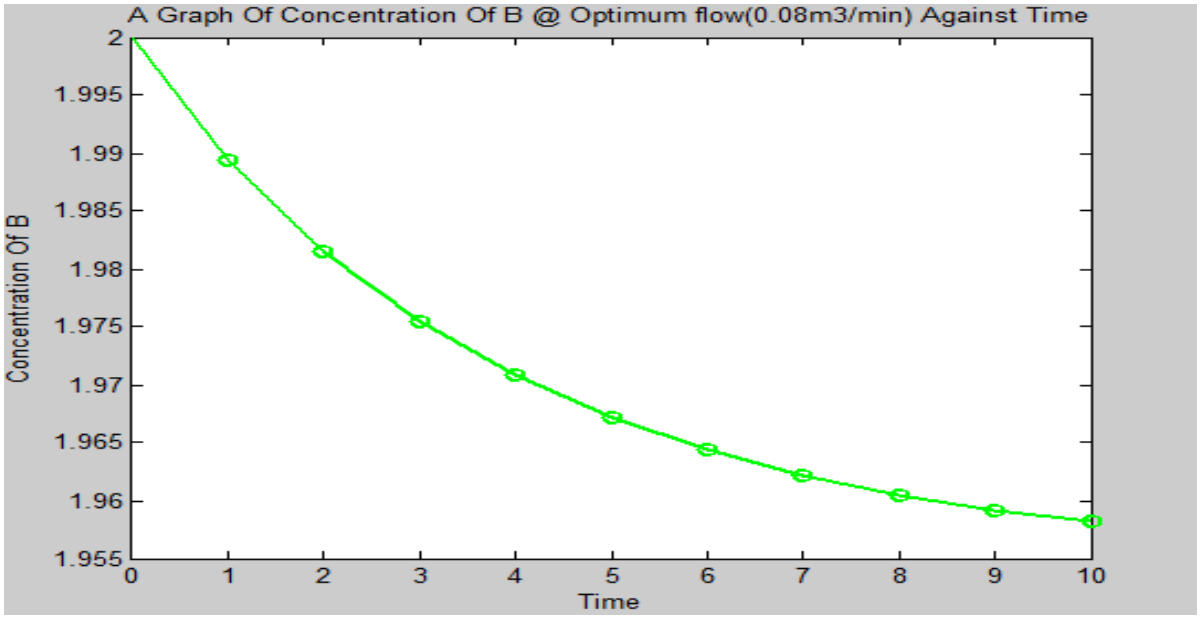

Figure 6: Plot of Variation in concentration of Water with time.

These figures show a decrease in the concentrations of both reactants as reaction proceeds. The validity of the models were ascertained using industrial data from the works of Batiha, (2004a) and comparing the results predicted from the model with industrial plant output. This comparison for the reactant's outputs are shown in Table 1.

Table 1: Comparison of Model Predictions and literature results

S/N	Component	Concentration ($kmol/m^3$)		% Deviation
		Model Prediction	Literature	
1.	Ethylene Oxide.	0.0582	0.0568	-2.47
2.	Water.	1.9582	1.9402	-0.93

Table 1 showed that the models accurately predicted the reactants outputs with a maximum deviation of 2.47%. Hence the models were used to simulate the behaviour of the product (Mono Ethylene Glycol) to fluctuations (changes) in the reactants inlet flowrate to the reactor. The behaviour of the CSTR (formation of the desired product, Mono-Ethylene Glycol (C_c)) to step-changes $\pm 25\%$ and $\pm 50\%$ in the feed flowrate F_i is shown in Figure 7.

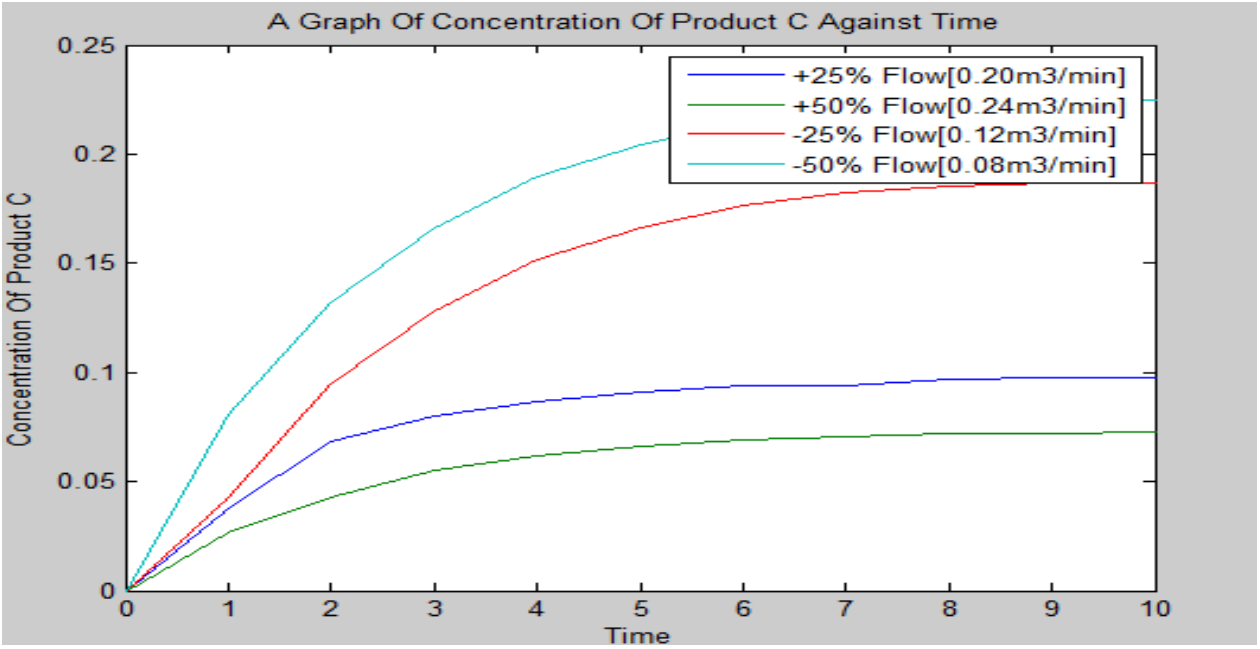

Figure 7: Effect of feed flow rate on the production rate of the desired product, MEG.

Figure 7 shows that the rate of formation of the desired product, Mono-Ethylene Glycol is greatly affected by fluctuations of the inlet feed volumetric flowrate.

3.2. Closed-Loop Response: Effect of the Controller

The closed-loop response of the process (the controlled variable – the amount/volume of MEG produced measure by the liquid/MEG height in the reactor) to (±) step changes in the inlet flowrate; (-) step changes are shown in Figures 8, 9 and 10 while (+) changes are shown in Figures 11, 12 and 13. The changes in inlet flowrate caused a decrease or an increase in the liquid level and are shown by the yellow lines in the figures. The closed loop responses of the liquid/MEG level in the reactor with a feedback PID controller at different values of its parameters aimed at stabilizing the liquid level are also shown in these figures. Some of the many iterations performed are hereby presented.

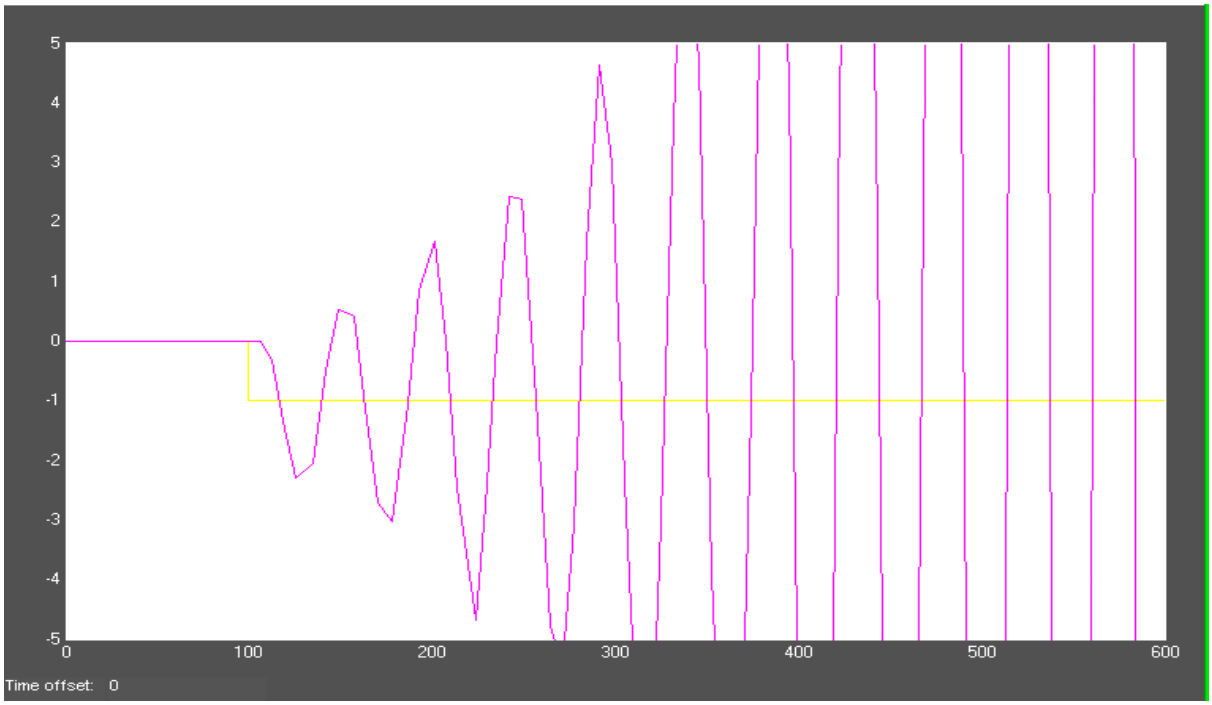

Figure 8: Effect of PID Controller at $\tau_I = 2$, and $\tau_D = 2$

Figure 8 shows fluctuations due to instabilities of the liquid level. The liquid level responded fast, oscillates progressively and continuously with increasing amplitude and a low period of oscillation. The process is quite unstable and the controller requires more tuning.

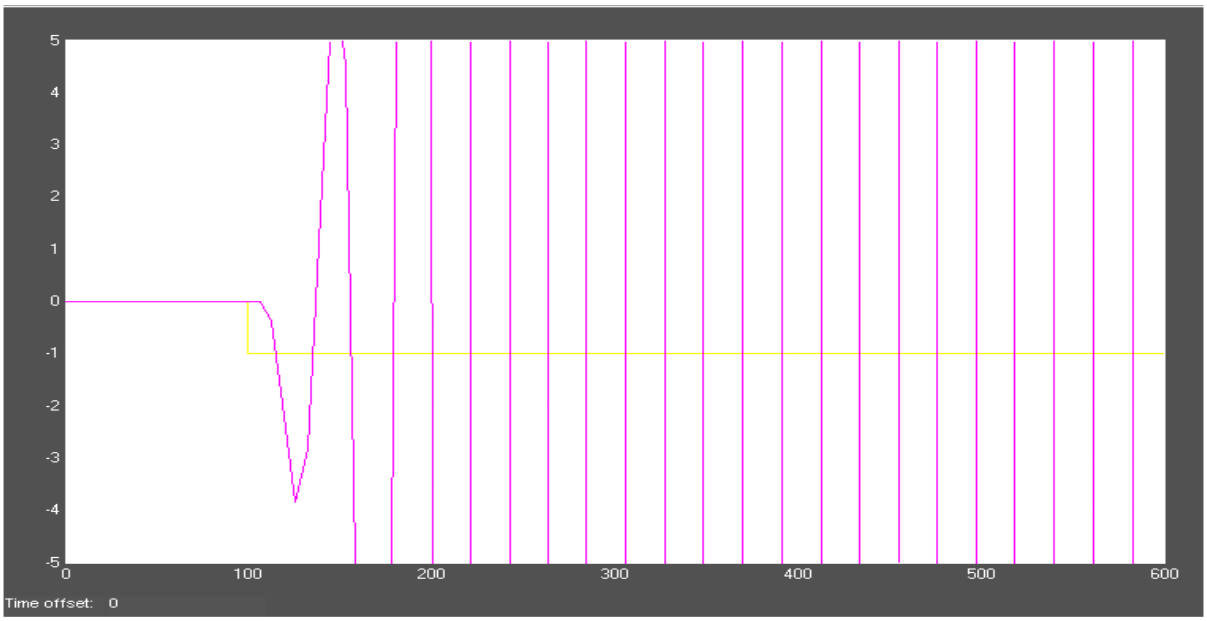

Figure 9: Effect of PID Controller at $\tau_I = 4$, and $\tau_D = 2$

In Figure 9, the liquid level response is slower, but still oscillates progressively and continuously with increasing amplitude and higher period of oscillation. The process is still unstable, with unbounded output and the controller requires more tuning.

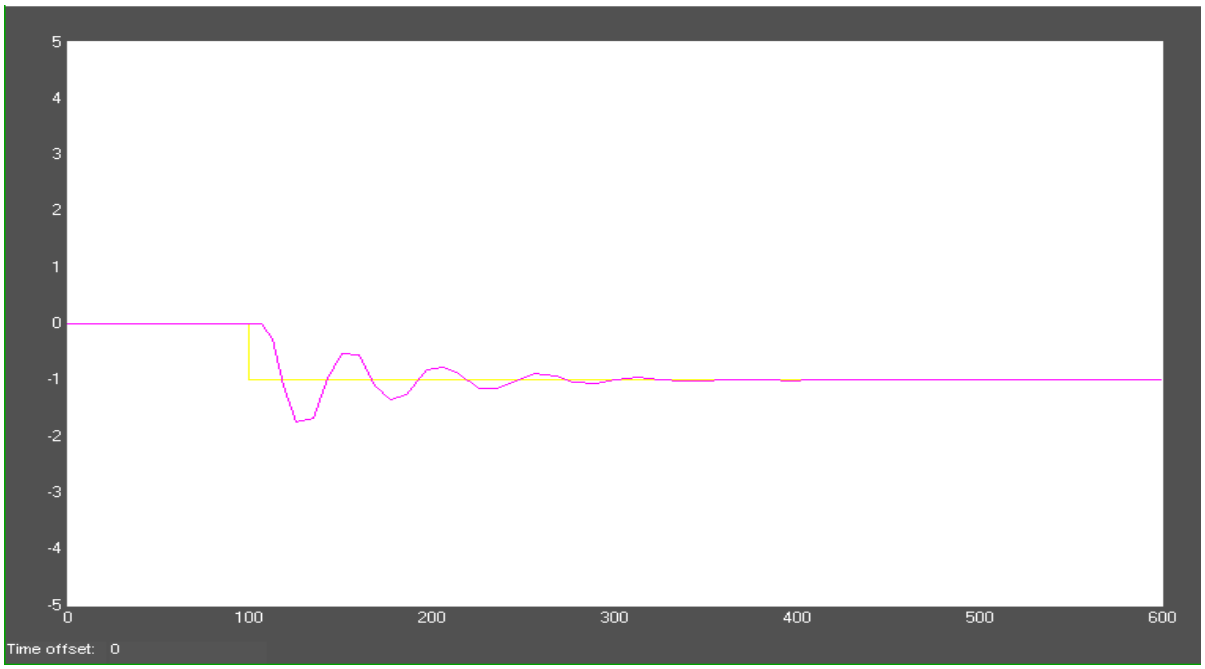

Figure 10: Effect of PID Controller at $\tau_I = 6$, and $\tau_D = 2$

Figure 10 shows that the liquid level response is a little sluggish, oscillates progressively with increasing amplitude, a smaller period of oscillation but attains stability after a time span of about 340 seconds.

These plots showed the effect of Integral Control in a composite control system such as a PID controller on the process. Results showed that for constant controller gain, K_C, as the integral time increases, the response becomes more sluggish, less oscillatory with lower overshoots and decay ratios.

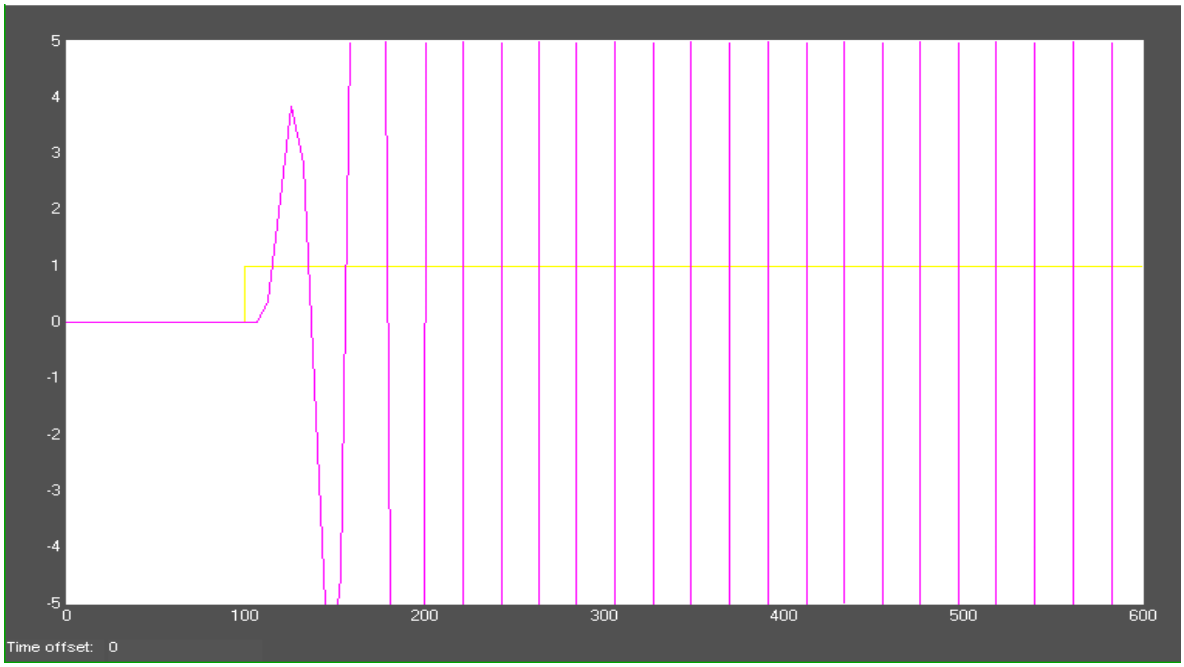

Figure 11: Effect of PID Controller at $\tau_I = 2$, and $\tau_D = 2$ for positive unit step-change

Figure 11 shows that the liquid level responded fast, oscillates progressively and continuously with increasing amplitude and a lower period of oscillation. The process is quite unstable and the controller requires more tuning.

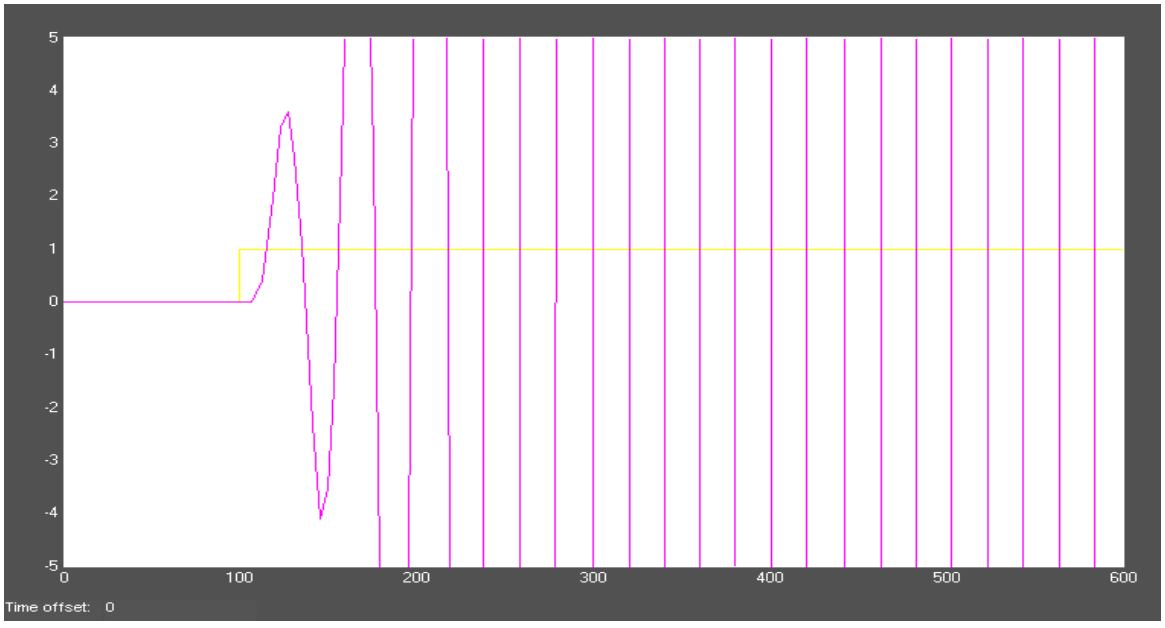

Figure 12: Effect of PID Controller at $\tau_I = 2$, and $\tau_D = 8$

Figure 12 shows that the liquid level responded a bit sluggish, oscillates progressively and continuously with increasing amplitude and a decrease in the overshoot. The process is quite unstable and the controller requires more tuning.

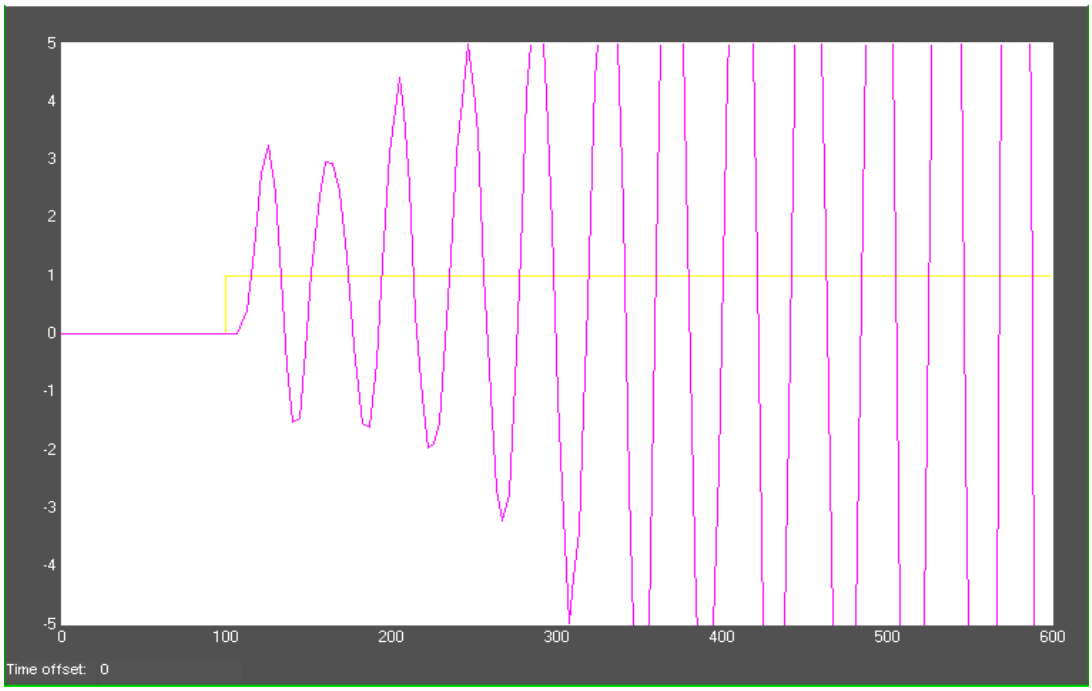

Figure 13: Effect of PID Controller at $\tau_I = 2$, and $\tau_D = 14$

Figure 13 shows that the liquid level response is more sluggish with a larger decrease in the overshoot. The process is still unstable.

Following the trends observed from the results of these plots, the integral and derivative time were further adjusted in a systematic/specific way to obtain the 'best' values of controller parameters for the process – values that gave faster and less oscillatory response that becomes stable in the shortest possible time. These are shown in Figures 14 and 15.

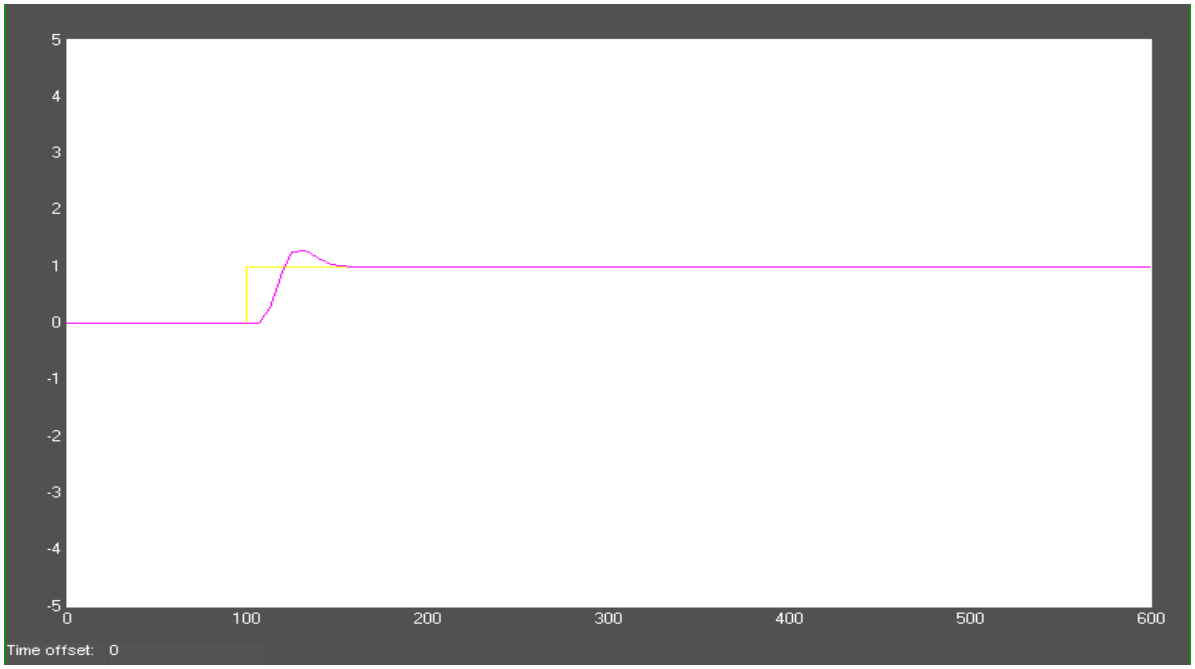

Figure 14: Effect of PID Controller at $\tau_I = 10$, and $\tau_D = 3$

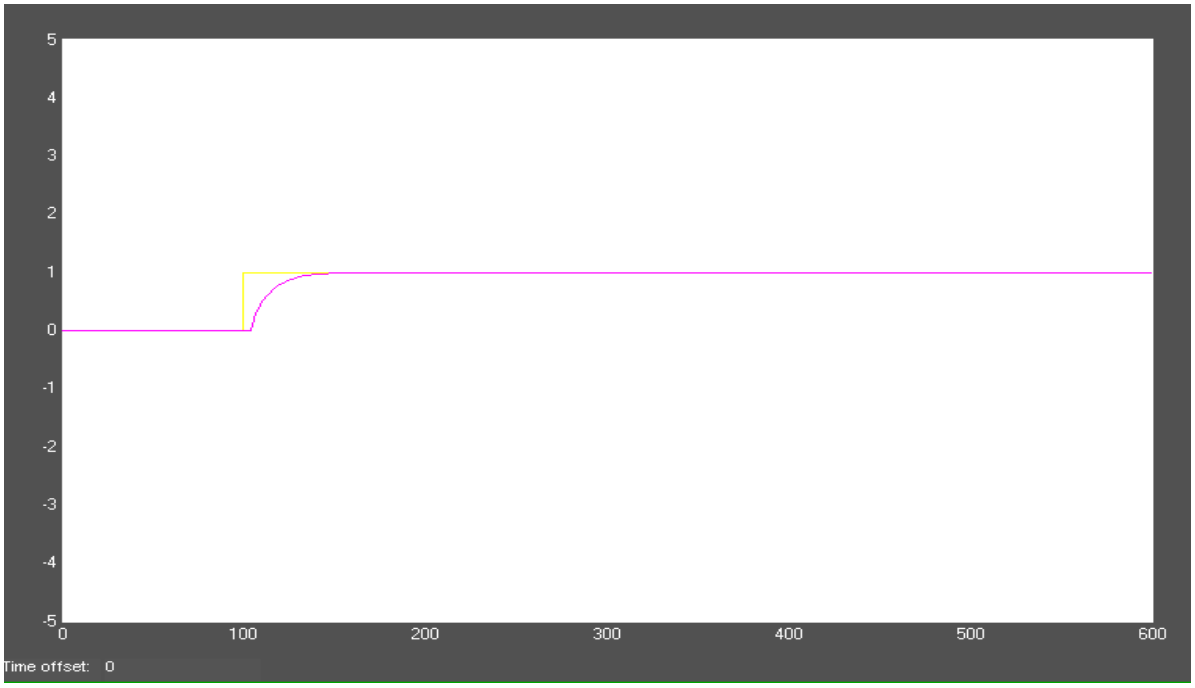

Figure 15: Effect of PID Controller at $\tau_I = 14$, and $\tau_D = 3$

These figures (14 and 15) show that by increasing the integral time to about 14 and the derivative time to 3 at a constant controller gain, the closed-loop response of the liquid level was almost stable. Therefore, the optimum values of the controller parameters that achieved the specified control objective were: $K_C = 0.1, \tau_I = 14, \tau_D = 3$

4. Conclusion

Dynamic models for the industrial process of the non-catalytic synthesis of Ethylene Glycol via the hydrolysis of Ethylene Oxide in a Continuos Stired Tank Reactor have been developed by applying the principles of conservation of mass and energy. The developed model equations were validated by solving the model equations with industrial plant data given by Batiha, (2004a). The model predictions of the reactants output obtained from the model compare favorably with industrial plant outputs with maximum deviation of 2.47%. Simulation of the continuous stired tank reactor to fluctuations/chamges in inlet feed flowrate showed a huge effect on the performance (volume of MEG produced) of the reactor. This justified the need for process control to maximize production and ensure selectivity towards the desired product. Process control was effected with a Proportional-Integral-Derivative feedback controller. A closed loop model (process with controller) was developed in terms of the transfer functions of the components of the closed loop block diagram. Solution of the closed loop model to step changes in the inlet flowrate showed oscillatory responce in the output (MEG level) with offset over a long period. Controller tunning was therefore performed using the on-line trial and error method to obtain optimum values of the controller parameters (controller gain K_C, the integral or reset time τ_I and the derivative time τ_D) of $K_C = 0.1, \tau_I = 14, \tau_D = 3$ which gave rapid and smooth responses to the set point changes with little or no oscillations and eliminated the offset (steady state error).

References

Arrieta, I. (2001). Ethylene Glycol. Retrieved from http://natsha.eng.usf.edu/gilbert/courses/modelandanalysis/portfolio_2001/1_project_1/arrieta_ethylene_glycol.pdf

Batiha, M. (2004a). Dynamic Modelling of the Non-Catalytic Process of Ethylene Oxide Hydrolysis, Journal of Science and Technology, Vol. 9 (1 & 2), pp. 17 – 27.

Batiha, M. (2004b). Kinetic Investigation of Consecutive-Parallel Reactions in the Non-Catalytic Process of Ethylene Oxide Hydrolysis, Journal of King Abdulaziz University: Engineering Science, Vol. 15, (1), pp. 19-31

Celik, F. E., Lawrence, H. & Bell, A. T. (2008). Synthesis of precursors to ethylene glycol from formaldehyde and methyl formate catalyzed by heteropoly acids, Journal of Molecular Catalysis A: Chemical 288, 87–96

Iwakura, T. & Miyagi, H. (2000.) US Patent 6147, 265.

Kawabe, K., (2000). US Patent 6080,897

Kruchten, V. (1999a). US Patent 5874,653

Kruchten, V. (1999b). WO Patent 9923,053.

Landau, R. & Ozero, B. J. (1982). Ethylene Glycol, Encyclopedia of chemical processing and Design. 2-52.

Li, Y., Yan, S., Yue, B., Yang, W., Xie, Z., Chen, Q. & He, H., (2004), Selective catalytic hydration of ethylene oxide over niobium oxide supported on α-alumina, Applied Catalysis A, General, 272, 1-2, 305 – 310.

Li, Y. C., Yan, S. R., Yang, W. M., Xie, Z. K., Chen, Q. L., Yue, B. & He, H. Y. (2005). Effects of support modification on $Nb_2O_5/\alpha\text{-}Al_2O_3$ catalyst for ethylene oxide hydration J. Mol. Catal. A: Chem., 226, 285–290.

Li, Y. C., Yan, S. R., Qian, L. P., Yang, W. M., Xie, Z. K., Chen, Q. L., Yue, B. & He, H. Y. (2006). Effect of tin on $Nb_2O_5/\alpha\text{-}Al_2O_3$ catalyst for ethylene oxide hydration, J. Catal. 241, 173-179.

Luyben, W. L. (1990). Process Modeling, Simulation and Control for Chemical Engineers, (2^{nd} ed.). Singapore, McGraw-Hill Publishing Company.

Melhem, S. A., Gianetto. A., Levin, M. E., Fisher, H. G., Chippett, S., Singh, S. K. & Chipman, P. I. (2001). Kinetics of the reactions of ethylene oxide with water and ethylene glycols, Process Safety Progress, 20, 4, 231 – 246.

Rebsdat, S. & Mayer, D. (2005). Ethylene oxide. In: Ullmann's Encyclopedia of Industrial Chemistry, 7th Ed., Weinheim, Wiley–VCH Publishers (on line)

Samoilov, N. A. & Mnushkin, I. A. (2012). Mathematical Modeling Fractionation Stage of Reactive Distillation Process for Production of Ethylene Glycol, Electronic Scientific Journal “Oil and Gas Business”, 4, 158 – 164.

Sinnott, R. & Towler, G. (2009). Chemical Engineering Design Volume 6. India: Elsevier Limited.

Stephanopoulos, G. (2012). Chemical Process Control: An Introduction to Theory and Practice. (Indian ed.). New Delhi, India: PHI Learning Private Limited.

Strickler G. R., Landon V. G., & Lee, G. J. (1999). US Patent WO1999031033A1.

Shvets, V. F., Kozlovskiy, R. A., Kozlovskiy, I. A., Makarov, M. G., Suchkov, J. P. & Koustov, A. V. (2005), The Model of Catalytic Reactor of Ethylene Glycol Production, Org. Process Res. Dev., 9 (6), 768 – 773.

Yang, G., Ren, N., Zhang, Y. & Tang, Y. (2010). Studies on mechanism for homogeneous catalytic hydration of ethylene oxide: Effects of pH window and esterification, Catalysis Communications 11, 447 – 450.

Numenclature

A = Cross Sectional Area (m^2)

C_{j_o} = Inlet Concentration of component j ($kmol/m^3$)

C_j = Outlet Concentration of component j ($kmol/m^3$)

E_i = Activation Energy for reaction path i (cal/g mol)

G_c = Transfer Function of the Controller

G_d = Transfer Function of the Load

G_f = Transfer Function of the Final Control Element

G_m = Transfer Function of the Measuring Device

G_p = Transfer Function of the Process (CSTR)

h = Height of Reactor (m)

i = Reaction path

j = Component

K_i = Reaction rate constant for reaction path i

K_{i_o} = Pre-exponential Factor for reaction path i $(m^3)^3\ kmol^{-3}S^{-1}$

q_i = Inlet Volumetric Flowrate of feed (m^3/min.)

q = Outlet Volumetric Flowrate of feed (m^3/min.)

r_j = Rate equation for component j

T_i = Inlet Temperature of feed (K)

T = Outlet Temperature (K)

V = Volume of Reactor (m^3)

C_p = Heat capacity of Feed (kJ $kmol^{-1}K^{-1}$)

ρ = Density of Feed (kg/m^3)

ΔH = Heat of Reaction for reaction (kJ $kmol^{-1}$)